2022 44th Annual International Conference of
the IEEE Engineering in Medicine & Biology Society (EMBC)
Scottish Event Campus, Glasgow, UK, July 11-15, 2022

2022 44th Annual International Conference of the IEEE Engineering in Medicine & Biology Society (EMBC) | 978-1-7281-2782-8/22/$31.00 ©2022 IEEE | DOI: 10.1109/EMBC48229.2022.9871694

System Design for Optimizing Drug Infusions Using Cardiovascular Space Mapping for Acute Heart Failure

Yasuyuki Kataoka[1], Yukiko Fukuda[1], Jon Peterson[1], Iris Shelly[1], Joe Alexander[1], Kenji Sunagawa[2]

***Abstract*— Acute heart failure is caused by various factors and requires multiple drug therapies to remedy underlying causes. Due to the complexity of pharmacologic effects of cardiovascular agents, few studies have theoretically addressed the multidrug optimization problem. This paper proposes a drug infusion system for acute heart failure that controls cardiovascular performance metrics (cardiac output, left atrial pressure, and mean arterial pressure) within desired ranges as dictated by the cardiovascular parameters (systemic vascular resistance, cardiac contractility, heart rate, and stressed blood volume). The key to our system design is modeling and controlling cardiovascular parameters to yield the desired cardiovascular metrics. A 'tailored drug infusion' technique controls parameters by solving the optimization problem in order to conquer the complexity of multi-dependencies and the different dosage limits among multiple drugs. A 'cardiovascular space mapping' technique identifies the desired parameters from the desired metrics by deriving the analytical solutions of the metrics as functions of the parameters. To facilitate clinical discussions, parameters were set to realistic values in 5,600 simulated patients. Our results showed not only that the optimized drug combinations and dosages controlled the cardiovascular metrics to within the desired ranges, but also that they mostly corresponded to the recommended clinical use guidelines. An additional value of our system is that it proactively predicts the limitations of the tailored drug therapy, which supports the clinical decision of pivoting to alternative treatment strategies such as mechanical circulatory support.**

I. Introduction

Patients with acute heart failure (AHF) are managed with pharmacological therapy to stabilize their hemodynamics. The selection of drugs is determined based on clinical findings and various examination results. In recent clinical practice, classes of cardiovascular agents, including diuretics, positive inotropes, vasopressors, and vasodilators are considered effective for treating AHF [1]–[3].

The complex underlying pathophysiologies of AHF and the unclear interactions and maximally tolerated dose ranges make it difficult to optimize drug therapy for each patient. In addition, because the patient's condition can easily fluctuate with slight changes in the infusion rate of these drugs, strict monitoring of the patient's condition and manual adjustments of drug dosages are required.

To reduce the burden of patient monitoring and manual interventions, several closed-loop systems have been developed to automatically adjust drug infusion rates to control the patient's arterial pressure (AP) and/or cardiac output (CO), while few studies are aiming to achieve optimal pharmacological therapy considering the patient's pathophysiologies, especially when the complexity of multiple drug use exists. [4]–[7].

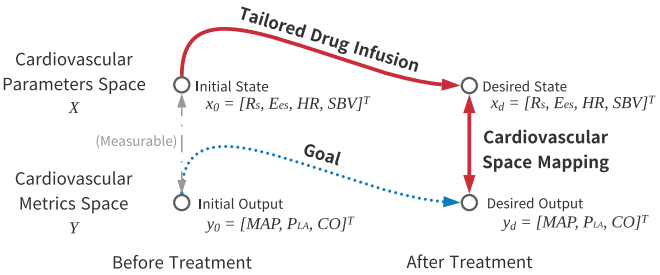

Fig. 1: Proposed Cardiovascular Control System Design

This paper proposes a drug infusion system for acute heart failure that optimally controls and maintains cardiovascular performance metrics (:=*CV metrics*): cardiac output (CO), left atrial pressure (P_{LA}), and mean arterial pressure (MAP) – within a desired range as dictated by the patient's cardiovascular parameters (:=*CV parameters*): systemic vascular resistance (R_s), cardiac contractility (E_{es}), heart rate (HR), and stressed blood volume (SBV). The inputs for the proposed system are multiple therapeutic drugs having different effects; the outputs are *CV metrics*. The inputs interact with the *CV parameters* to determine the *CV metrics*.

Our proposed methods involve two key techniques, as shown in Fig. 1, where the *CV parameters* space and the *CV metrics* space are denoted by X and Y, respectively. The first technique is designed to tackle the complexity of multiple drug infusions: multi-dependencies and different dosage limitations. This *tailored drug infusion* method optimizes the drug combination and dosage from the initial state of heart failure into the desired state of stable hemodynamics within the *CV parameters* space ($x_0 \in X \rightarrow x_d \in X$) via a linear programming formulation using a drug infusion model. Here, one challenge is identifying the control target, i.e., the desired *CV parameters* that correspond to the desired *CV metrics*. The second technique is designed to address this inverse problem. This *cardiovascular space mapping* method identifies the desired *CV parameters* from the desired *CV metrics* ($y_d \in Y \rightarrow x_d \in X$) via the derived analytical solution of P_{LA} and CO as functions of *CV parameters*. We applied *Guyton's Venous Return Curve* to the pulmonary circulation, then analytically solved its intersection with the *Frank-Starling Curve* of the left ventricle.

In simulation experiments, the parameters are set to rea-

[1] NTT Research, Inc., 940 Stewart Dr, Sunnyvale, 94085 CA, USA {yasuyuki.kataoka, yukiko.fukuda, jon.peterson, iris.shelly, joe.alexander}@ntt-research.com
[2] Circulatory System Research Foundation, 4F 3-24-6 Hongo Bunkyo Ku, Tokyo, 113-0033, Japan sunagawa.kenji.310@m.kyushu-u.ac.jp

listic values to facilitate clinical discussions and exploration of actionable insights that support the treatment of AHF. Our results showed not only optimized drug combinations and dosages but also revealed the limitations of these drug treatments. Such information can provide clinical decision-making support for a clinician to pivot proactively from drug treatments to mechanical interventions.

II. Methods

A. Cardiovascular Parameter Control System Design

Drugs directly affect *CV parameters* based on their pharmacology. Changes in *CV parameters* will in turn affect *CV metrics*. Thus, the key to our system design is modeling and controlling *CV parameters* values to yield the desired outputs in terms of *CV metrics*.

In our system, let x denote the *CV parameters* $x := [R_s, E_{es}, HR, SBV]^T \in R^4$. Assuming x is measurable, the patient's initial *CV parameters* x_0 are given. Next, let the input u be the drug infusion $u := [u_1, \cdots, u_5]^T \in R^5$ as described in TABLE I. The infusion drugs were selected to represent key classes used in treatment of AHF: Dobutamine (DOB) as a positive inotrope, Norepinephrine (NE) as a vasopressor, Sodium Nitroprusside (SNP) as a vasodilator, Dextran (DEX) as a fluid, and Furosemide (FRO) as a diuretic. Then, let y be the *CV metrics* $y := [MAP, P_{LA}, CO]^T$.

The following two subsections will introduce the two techniques shown in Fig. 1. The first technique, *tailored drug infusion*, optimizes the drug combination and dosage that converts the initial *CV parameters* $x_0 \in X$ of AHF patient into the desired one $x_d \in X$ via a linear programming formulation using the drug infusion model. The second technique, *cardiovascular space mapping*, identifies the control target $x_d \in X$ from the desired output $y_d \in Y$.

B. Tailored Drug Infusion ($x_0 \in X \rightarrow x_d \in X$)

Firstly, this proposed technique models the multi-dependencies of simultaneous multiple drug infusion when drug effects have converged. The assumptions in this model are a) each drug functions to add its effects linearly to influence *CV parameters* and b) cross-terms of the multiple inputs, e.g., $u_1 \times u_2$ are not considered. Then, our drug infusion model becomes

$$x = Bu + x_0 \tag{1}$$

where x shows the *CV parameters* following drug infusion, once updated and converged. The input matrix B is the drug library that represents the multi-dependency effect from each drug to *CV parameters*. In the case of our drug inputs, the drug library matrix is represented by

$$B = \begin{bmatrix} 0 & k_{12+} & k_{13-} & 0 & 0 \\ k_{21+} & k_{22+} & 0 & 0 & 0 \\ 0 & 0 & 0 & 0 & 0 \\ k_{41+} & 0 & k_{43-} & k_{44+} & k_{45-} \end{bmatrix}$$

based on known pharmacological effects [2], [8]. Each element is equivalent to the gain, and the plus or minus sign indicates the direction of the change. For example, drug input u_3 (Sodium Nitroprusside) decreases R_s and SBV, as shown by the gains k_{13-} and k_{43-}.

TABLE I: Intervention Drugs for AHF Treatment

Input	Name	Abb.	Max Dose	Unit
u_1	Dobutamine	DOB	10	[μg/kg/min]
u_2	Norepinephrine	NE	3	[μg/kg/min]
u_3	Nitroprusside	SNP	10	[μg/kg/min]
u_4	Dextran	DEX	25	[ml/kg]
u_5	Furosemide	FRO	180	[mg]

The above-simplified model decribes a set of linear simultaneous equations to compute the *CV parameters* when drugs are infused. Thus, the input optimization problem with the input dosage limitations can be formulated by a linear programming problem:

$$\begin{aligned} &\text{Minimize} \\ &\quad w^T u^* \\ &\text{subject to} \\ &\quad x_d - x_0 = Bu^* \\ &\quad 0 \le u^* \le \bar{u} \end{aligned} \tag{2}$$

where u^* is the optimal input that minimizes the total dosage of the drug use with the designed weight $w = [w_1, \cdots, w_5]^T$ and $\bar{u}$ is the dosage limitation.

C. Cardiovascular Space Mapping ($y_d \in Y \rightarrow x_d \in X$)

1) Analytical Solution ($X \rightarrow Y$): We derived the analytical solution that maps the *CV parameter* space X to the *CV metrics* space Y using approximation. This was derived from the intersection of the *Frank-Starling Curve* and *Guyton's Venous Return Curve* formula [9], [10].

Firstly, the *Frank-Starling Curve* defines the relationship between CO and P_{LA}. The mechanics of the *Frank-Starling Curve* derived in [11] shows

$$CO = \frac{HR \cdot E_{es}}{\beta(E_{es} + \frac{HR}{60} \cdot R_s)} \cdot \ln \frac{P_{LA} + \alpha}{\alpha} \quad \left[\frac{\text{ml}}{\text{min}}\right] \tag{3}$$

where heart rate (HR), systemic vascular resistance (R_s), and left ventricular contractility (E_{es}) are the given *CV parameters* and α and β are constant parameters to define the end-diastolic pressure-volume relationship (EDPVR) [12]. In (3), EDPVR is assumed to be

$$P_{ed} = \alpha \left(\exp\{\beta(V_{ed} - V_0)\} - 1\right) \tag{4}$$

$$\Leftrightarrow V_{ed} = \frac{1}{\beta} \ln \frac{P_{ed} + \alpha}{\alpha} + V_0 \text{ [ml]}. \tag{5}$$

Note that P_{ed} is left ventricular end-diastolic pressure and is equivalent to P_{LA} in the filling phase.

Secondly, we applied *Guyton's Venous Return Curve* to the pulmonary circulation [10], [13],

$$CO = \frac{1}{R_{vp}} \left(\frac{V_p}{C_p} - P_{LA}\right) \quad \left[\frac{\text{ml}}{\text{sec}}\right] \tag{6}$$

where R_{vp} is the resistance for pulmonary venous return, and where C_p and V_p are the compliance and the stressed blood volume in the pulmonary circulation, respectively. Assuming

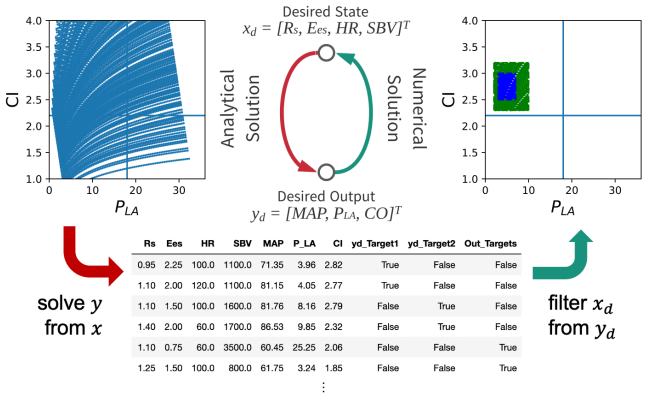

Fig. 2: Schema of *Cardiovascular Space Mapping*

that total stressed blood volume (SBV) is distributed by the compliance ratio of the systemic and pulmonary circulation, V_p is given by

$$V_p \approx \frac{C_p}{C_s + C_p} SBV \tag{7}$$

where C_s is the compliance of the systemic circulation. Substituting V_p in (6) with (7) yields

$$CO = \frac{1}{R_{v_p}} \left(\frac{SBV}{C_p + C_s} - P_{LA} \right) \left[\frac{\text{ml}}{\text{sec}} \right]. \tag{8}$$

Thirdly, solving (3) and (8) with respect to (P_{LA}, CO), the analytical solution of P_{LA} and CO is given by

$$P_{LA} = -\alpha \left(\frac{aW\left(-\frac{b}{a}\exp\left(\frac{c}{a}\right)\right)}{b} \right) - \alpha \text{ [mmHg]} \tag{9}$$

$$CO = -aW\left(-\frac{b}{a}\exp\left(\frac{c}{a}\right)\right) + c \left[\frac{\text{L}}{\text{min}} \right] \tag{10}$$

where $W(\cdot)$ is defined as the Lambert function and

$$a = \frac{1}{1000} \frac{HR \cdot E_{es}}{\beta(E_{es} + \frac{HR}{60} \cdot R_s)} \tag{11}$$

$$b = -\frac{60}{1000} \frac{\alpha}{R_{vp}} \tag{12}$$

$$c = \frac{60}{1000} \frac{1}{R_{vp}} \left(\frac{SBV}{C_s + C_p} + \alpha \right). \tag{13}$$

2) Numerical Solution ($y_d \in Y \rightarrow x_d \in X$): The inverse problem of computing the mapping function $Y \rightarrow X$ is intrinsically difficult due to the inverse nonlinear relationships between the two spaces and their dimensional difference. A conceptual representation behind the solution to compute the desired *CV parameter* x_d is shown in Fig. 2.

Firstly, leveraging the analytical solution (9) and (10) makes it efficient to simulate various patient scenarios and outcomes. These simulations provide many pairs of diverse *CV parameters* x and their resulting *CV metrics* y. These computed pairs are stored in a database.

Secondly, by filtering the database by y_d in the target region, our method can identify the set of desired *CV parameters* x_d. In this filtering process, another constraint can be applied for MAP (mean arterial pressure) which is given by

$$MAP = CO \cdot R_s. \tag{14}$$

TABLE II: Constant Parameters used in Experiments

Const.	Value	Unit ($\gamma = \mu$g/kg/min)	Description
k_{12+}	0.100	[(mmHg.s)/(γ.ml)]	NE $\rightarrow R_s$
k_{13-}	-0.211	[ml/(γ.kg)]	SNP $\rightarrow R_s$
k_{21+}	0.0625	[mmHg/(γ.ml)]	DOB $\rightarrow E_{es}$
k_{22+}	0.050	[mmHg/(γ.ml)]	NE $\rightarrow E_{es}$
k_{41+}	0.339	[ml/(γ.kg)]	DOB $\rightarrow SBV$
k_{43-}	-1.430	[ml/(γ.kg)]	SNP $\rightarrow SBV$
k_{44+}	1.000	[ml/ml]	DEX $\rightarrow SBV$
k_{45-}	-0.400	[ml/(mg.kg)]	FRO $\rightarrow SBV$
α	0.440	unitless	EDPVR
β	0.030	unitless	EDPVR
C_p	18.6	[ml/mmHg]	Pulmonary Compliance
C_s	102.0	[ml/mmHg]	Systemic Compliance
R_{vp}	0.0686	[mmHg.sec/ml]	Pulmonary VR Resistance
$w_{1\cdots4}$	1.0	unitless	weights w in (2)
w_5	0.1	unitless	weight w in (2)

TABLE III: Control Targets in *CV metrics* space Y

	MAP	P_{LA}	CI
Target 1	[70.0, 106.7]	[3.0, 7.0]	[2.5, 3.0]
Target 2	[70.0, 106.7]	[2.0, 10.0]	[2.3, 3.2]

III. Simulation Results

A. Setting

The constant parameters are set as shown in TABLE II based on our best available knowledge from [8] to support clinical discussions even with simulated data. Although choices of particular values may be arguable, the proposed methods remain the same.

1) Exp.1 Treatability Analysis: The simulated AHF patients are assumed to have different *CV parameters* values formed as all combinations of $R_s = [0.80 : 0.15 : 1.40]$, $E_{es} = [0.75 : 0.25 : 2.50]$, $HR = [60 : 20 : 120]$, and $SBV = [600 : 100 : 4000]$, generating a total of 5,600 patients.

The desired outcome $y_d \in Y$ is computed based on the two target *CV metrics* ranges shown in TABLE III. Here, cardiac index (CI [L/min/m^2] := CO/BSA, BSA: body surface area) is considered for assessing the *Forrester Classification* [14] where the horizontal axis is P_{LA} and the vertical axis is CI. BSA was fixed at an average value of 1.6 [m^2]. The range of MAP is a common prerequisite for both control targets. Given the desired outcome y_d, the desired *CV parameter* x_d was derived by our proposed method of *cardiovascular space mapping*. Then, the optimized input u^* was computed by our other proposed method of *tailored drug infusion* that converts x_0 to x_d. In this simulation experiment, the design parameter of the weight w_5 is set to 0.1 to favor use of FRO over SNP to decrease SBV. If the linear programming problem solution is feasible to at least one x_d in *Target 1*, then the patient is *treatable* to *Target 1*.

TABLE IV: Statistics of the Simulated Patients Before Drug Infusion in *Forrester Classification*

	R_s	E_{es}	HR	SBV	MAP	P_{LA}	CI
Subset I (warm & dry)	1.07±0.21	1.83±0.50	94.42±21.52	2011.73±590.91	87.88±22.05	10.96±4.28	3.12±0.68
Subset II (warm & wet)	1.10±0.21	1.62±0.55	89.05±22.28	3483.58±341.05	100.85±25.14	22.50±2.72	3.49±0.78
Subset III (cold & dry)	1.15±0.20	1.30±0.54	83.41±22.11	1154.73±518.55	54.90±12.04	6.29±4.13	1.79±0.27
Subset IV (cold & wet)	1.29±0.13	0.79±0.09	76.88±20.32	3231.21±418.01	69.03±7.35	23.12±3.41	2.01±0.14

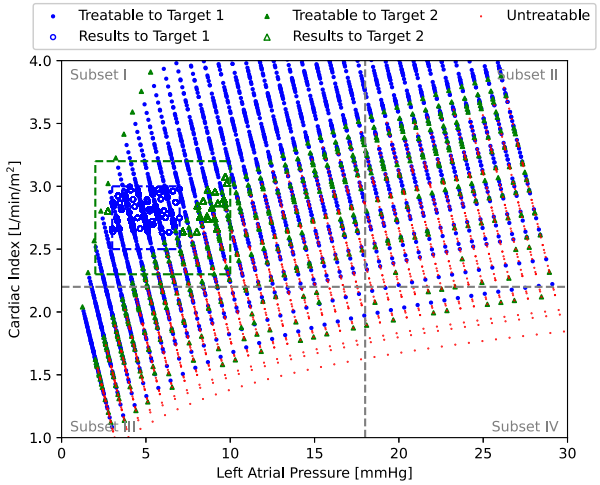

Fig. 3: Treatability of 5,600 Patients on (P_{LA}, CI) [*Exp.1*]

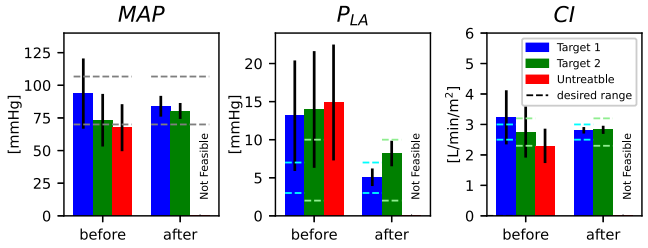

Fig. 4: Control Results by *CV metrics* y [*Exp.1*]

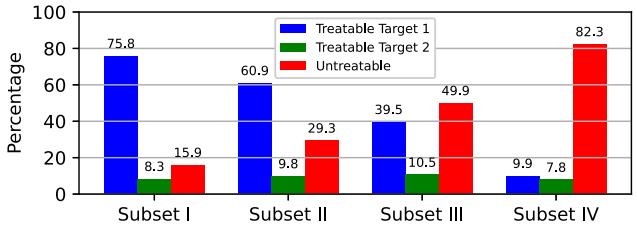

Fig. 5: Treatable Probability by Subsets [*Exp.1*]

If the patient is not *treatable* to *Target 1* and the solution is feasible to at least one x_d in the *Target 2*, then the patient is considered *treatable* to *Target 2*. Otherwise, the patient is considered *untreatable*. To save on the computational expense of this experiment, two hundred x_d in each control target were chosen randomly.

2) Exp.2 Pathophysiological Scenario Analysis: This simulation experiment investigates how our tailored drugs function in specific clinical scenarios. The following scenarios were thoroughly studied in *Forrester Classification* Subsets II, III and IV. To investigate the outcomes of *tailored drug infusion*, all of the x_d in each target range are tested, meaning multiple solutions of tailored drug infusion can be computed from one patient in *Exp.2*.

1) warm and wet patient in Subset II
   $x_0 : [R_s = 1.4, E_{es} = 2.5, HR = 80, SBV = 3500]$
2) cold and dry patient in Subset III
   $x_0 : [R_s = 1.0, E_{es} = 1.5, HR = 100, SBV = 800]$
3) cold and wet patient in Subset IV
   $x_0 : [R_s = 1.4, E_{es} = 0.75, HR = 120, SBV = 2700]$

B. Results

1) Exp.1: The results of *Exp.1 Treatability Analysis* validated that the proposed optimal drug infusion system can treat the initial *CV metrics* to within the desired range. The outcomes of 5,600 patients are shown in Fig. 3. In this experiment, our proposed methods resulted in 3,465 patients treatable within the bounds of *Target 1*, 515 patients treatable within the bounds of *Target 2*, and 1,620 untreatable patients.

The gray dashed lines in Fig. 3 indicate the boundaries separating *Forrester Classification* Subsets according to degree of patient perfusion and pulmonary congestion; these are, Subset I (warm & dry), Subset II (warm & wet), Subset III (cold & dry), and Subset IV (cold & wet). The *CV parameters* and *CV metrics* before the drug infusion are shown in TABLE IV.

Both Fig. 3 and Fig. 4 clearly show a favorable result in terms of *CV metrics* in that treatable patients were transitioned into the target region.

2) Exp.2: The results of *Exp.2 Pathophysiological Scenario Analysis* are shown in Fig. 6 and describe how our tailored drug infusion performed in each pathophysiological scenario. The corresponding results for *CV parameters* are shown in Fig. 7. These results will be discussed from a clinical perspective about how tailored drug therapy relates to standard clinical treatments for these categories of AHF patients.

IV. Discussion

1) Exp.1: Firstly, the 5,600 patients before drug infusion are discussed. From TABLE IV, the mean P_{LA} and CI values of each Subset indicate that all patients are well assigned to the four Subsets. In addition, volume overload (increased SBV) is prominent in the 'wet' Subsets (Subsets II and IV), while low perfusion (decreased MAP) is seen in the 'cold' Subsets (Subsets III and IV). All these features are consistent with clinical findings and underlying pathophysiologies.

Next, the use of different interventions for untreatable patients is discussed. The probability of *treatability* is shown in Fig. 5. Our simulation indicates that the largest percentage

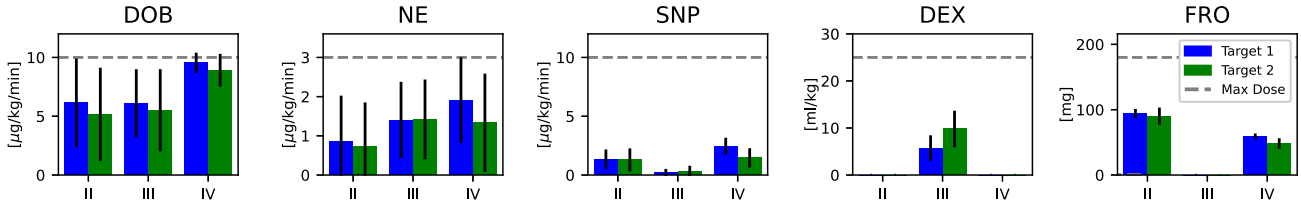

Fig. 6: Tailored Drug Infusion for each Scenario in Subset II, III, and IV [*Exp.2*]

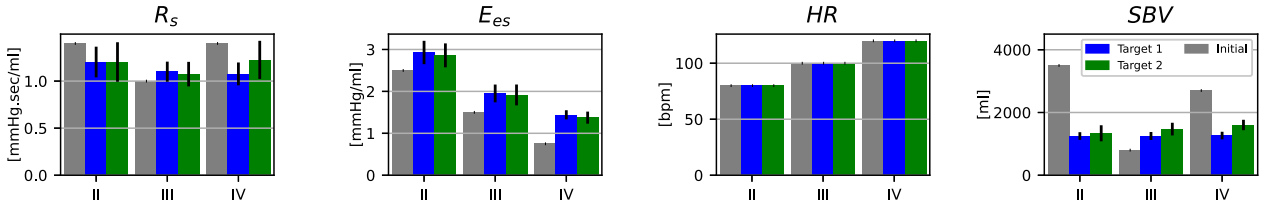

Fig. 7: Cardiovascular Parameter Change via Tailored Drug Infusion for each Scenario in Subset II, III, and IV [*Exp.2*]

of untreatable patients is in Subset IV. The *untreatable* patients can be interpreted as patients who will require advanced management beyond drug therapy - i.e., mechanical circulatory support.

According to the study of patients in the cardiac intensive care unit by *Forrester Classification* [15], the patients in Subset IV needed invasive interventions, e.g., left ventricular assist device (LVAD) or intra-aortic balloon pump (IABP), more frequently than the other patients in different Subsets. In contrast, several percent of patients, even in Subset I, needed invasive (or advanced) interventions. Our result similarly implied that a patient in any Subset may need other therapeutics beyond drug treatment. Thus, proactive decision-making support for physicians to switch intervention therapy should be carefully determined by each patient's pathophysiological scenario.

This pivotal decision has been one of the critical challenges in clinical settings in managing AHF [16]. Our methods and simulation results can assist in this challenge. Firstly, our methods can judge the *treatability* for each patient scenario even in an anomalous case in any Subset of *Forrester Classification*, e.g., an untreatable case in Subset I. Our method can simulate *treatability* by adjusting the design parameters in our methods: control target region, drug combinations, or the weight w in the objective functions. Secondly, it is possible to create a *treatability* classifier by machine learning approach whose labeled data could be our simulated data samples, i.e., *CV parameters* and *CV metrics* for the features and the resulting *treatability* for the label. This data-driven approach has the potential to make the classifier more accurate than our present proposal because it can unify the real patient's data in addition to our simulated labeled data.

2) Exp.2: We simulated three different scenarios to investigate whether the optimal drug combinations were correctly used in accordance with present clinical practice. Firstly, diuretics and/or vasodilators are the first-line drugs for patients with pulmonary congestion. As shown in Fig. 6, it was confirmed that FRO and SNP were used in Subsets II and IV (wet). In contrast, fluid replenishment is the first-line treatment if a patient is evaluated to be in a hypovolemic state, and our system provided adequate DEX for Subset III. Secondly, positive inotropes are recommended for AHF patients with low cardiac output (cold) in clinical practice, while our experiment indicated DOB was used in all Subsets. This can be explained as follows: a) DOB was used to improve CI in cold patients by increasing their E_{es} (direct effect), and b) DOB decreased P_{LA} in wet patients by increasing CO (indirect effect) according to (8). The direct effect of DOB is well known in clinical practice, while our result additionally demonstrated the beneficial indirect effect of DOB for pulmonary congestion. Finally, a vasopressor is considered in clinical settings with low blood pressure when the response of fluid resuscitation is inadequate. However, in our simulation, NE was administered to Subset II patients with elevated MAP, which was not in accordance with the clinical guidelines. This inconsistency can be addressed within our system, for example by more heavily weighing the penalty for the use of NE by adjusting the design parameter w_2 in (2).

Regarding optimal inputs, our system found that most of the treatable patients could be transitioned into multiple cardiovascular states within the target regions. It would be beneficial to further optimize tailored drug infusions among the multiple feasible solutions in order to identify the most optimal single solution. For example, there could be an additional objective function, $\sum_i u_i/\bar{u}_i$ that minimizes the sum of the dosage ratios for each drug. The results of such an additional optimization for each scenario are shown in Fig. 8. Indeed, this result corresponds to the drug choices in the *Forrester Classification* guideline. It is noteworthy that the objective function can be set flexibly for any of the various objectives of drug treatment for each clinical situation. For example, minimizing the myocardial oxygen consumption (MVO_2) is crucial in reducing the risk of ischemia. Our proposed approach is designed to accommodate new drugs such as β*-blockers* which decrease HR and E_{es}. While decreasing HR helps minimize MVO_2, decreasing E_{es} also lowers CO. Thus, leveraging β*-blockers* to treat AHF is a challenging task in the present clinical practice. As a next

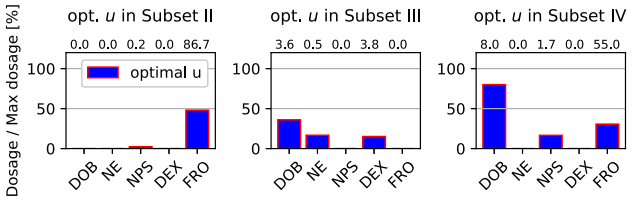

Fig. 8: Optimized Drug Use among Treatable Solutions

step, our system should be evaluated in the context of different optimization problems for various clinical scenarios.

3) Limitation: In this study, we obtained the analytical solution assuming that the proportion of the volume of systemic circulation and pulmonary circulation remains constant in heart failure. However, this proportion depends on the functional balance between the left and right ventricles. Applying the generalized circulatory equilibrium framework [13] would help develop our analytical solution.

The present simulation assumes the simultaneous administration of multiple drugs. Pharmacokinetics, e.g., the onset of action and peak effect, are not considered. Needless to say, dynamic drug responses should be incorporated into the analysis to simulate the time course of realistic drug interventions.

In the human cardiovascular system, multiple regulatory systems stabilize hemodynamics. One of the most powerful regulatory systems is sympathetic cardiovascular regulation via the baroreflex system. In this study, we did not implement the baroreflex system. However, various studies have demonstrated the quantitative influence of the baroreflex on *CV parameters*. Such observations allow us to implement the sympathetic nervous system in our future model.

V. Conclusion

In this paper, we have proposed a drug infusion system for acute heart failure. The key to our system design is the modeling and controlling of *CV parameters* to yield *CV metrics* within a desired range. The *tailored drug infusion* technique controls parameters by conquering multi-dependencies and different dosage limits among various drugs. The *cardiovascular space mapping* technique identifies the desired parameters from the desired metrics.

Our simulation results of 5,600 different scenarios showed not only that the optimized drug combinations and dosages successfully controlled the cardiovascular metrics to within the desired ranges but also that they mostly corresponded to the recommended drug clinical use guidelines. Importantly, our methods also were able to identify limits on response to drug therapy, which supports the clinical decision of pivoting to treatment strategies that may include mechanical interventions.

Our next steps will be to investigate how robustly our system can be adapted to meet additional clinical requirements such as the addition of drugs with potentially more complex interactions and less well-characterized on- and off-target pharmacological effects; or to address the clinical need for minimizing myocardial oxygen consumption also in patients with acute heart failure.

References

[1] R. J. DiDomenico, H. Y. Park, M. R. Southworth, H. M. Eyrich, R. K. Lewis, and e. a. Finley, "Guidelines for Acute Decompensated Heart Failure Treatment," *Annals of Pharmacotherapy*, vol. 38, no. 4, pp. 649–660, 2004.

[2] C. B. Overgaard and V. Džavík, "Inotropes and vasopressors," *Circulation*, vol. 118, no. 10, pp. 1047–1056, 2008.

[3] M. S. Nieminen, M. Böhm, M. R. Cowie, H. Drexler, G. S. Filippatos, G. Jondeau, and et al., "Executive summary of the guidelines on the diagnosis and treatment of acute heart failure: The Task Force on Acute Heart Failure of the European Society of Cardiology," *European Heart Journal*, vol. 26, no. 4, pp. 384–416, 2005-01.

[4] C. Yu, R. Roy, H. Kaufman, and B. Bequette, "Multiple-model adaptive predictive control of mean arterial pressure and cardiac output," *IEEE transactions on bio-medical engineering*, vol. 39, no. 8, pp. 765–778, 1992.

[5] J. Alexandre, C. Dragos, V. d. L. Philippe, B. Luc, A. Brenton, D. Jacques, and et al., "Automated closed-loop versus manually controlled norepinephrine infusion in patients undergoing intermediate- to high-risk abdominal surgery: a randomised controlled trial," *British journal of anaesthesia*, vol. 126, no. 1, pp. 210–218, 2021.

[6] K. Uemura, M. Sugimachi, T. Kawada, and K. Sunagawa, "Automated drug delivery system for the management of hemodynamics and cardiac energetic in acute heart failure," *32nd Annual International Conference of the IEEE EMBSB*, vol. 2010, pp. 5222–5, 2010.

[7] K. Kashihara, "Automatic Regulation of Hemodynamic Variables in Acute Heart Failure by a Multiple Adaptive Predictive Controller Based on Neural Networks," *Annals of Biomedical Engineering*, vol. 34, no. 12, pp. 1846–1869, 2006.

[8] K. Uemura, A. Kamiya, I. Hidaka, T. Kawada, S. Shimizu, T. Shishido, and et al., "Automated drug delivery system to control systemic arterial pressure, cardiac output, and left heart filling pressure in acute decompensated heart failure," *Journal of Applied Physiology*, vol. 100, no. 4, pp. 1278—1286, 2006.

[9] A. C. Guyton, "Determination of cardiac output by equating venous return curves with cardiac response curves," *Physiological reviews*, vol. 35, no. 1, pp. 123–9, 1955.

[10] A. C. Guyton, A. W. Lindsey, B. Abernathy, and T. Richardson, "Venous Return at Various Right Atrial Pressures and the Normal Venous Return Curve," *American Journal of Physiology-Legacy Content*, vol. 189, no. 3, pp. 609–615, 1957.

[11] K. Sunagawa, W. L. Maughan, D. Burkhoff, and K. Sagawa, "Left ventricular interaction with arterial load studied in isolated canine ventricle," *American Physiological Society*, vol. 245, no. 5 Pt 1, pp. H773–80, 1983.

[12] D. Burkhoff, I. Mirsky, and H. Suga, "Assessment of systolic and diastolic ventricular properties via pressure-volume analysis: a guide for clinical, translational, and basic researchers," *American Journal of Physiology-Heart and Circulatory Physiology*, vol. 289, no. 2, pp. H501–H512, 2005.

[13] K. Uemura, M. Sugimachi, T. Kawada, A. Kamiya, Y. Jin, K. Kashihara, and et al., "A novel framework of circulatory equilibrium," *American Journal of Physiology-Heart and Circulatory Physiology*, vol. 286, no. 6, pp. H2376–85, 2004.

[14] J. S., Forrester, G. A., Diamond, and S. H.J.C., "Correlative classification of clinical and hemodynamic function after acute myocardial infarction," *American Journal of Cardiology*, vol. 39, no. 2, pp. 137–145, 1977.

[15] K. Kim, J. C. Jentzer, B. M. Wiley, W. R. Miranda, C. Bennett, G. W. Barsness, and et al., "Diamond–Forrester classification using echocardiography haemodynamic assessment in cardiac intensive care unit patients," *Diamond-Forrester classification using echocardiography haemodynamic assessment in cardiac intensive care unit patients*, vol. 8, no. 6, pp. 4933–4943, 2021.

[16] T. M. Maddox, J. L. Januzzi, L. A. Allen, K. Breathett, J. Butler, L. L. Davis, and et al., "2021 Update to the 2017 ACC Expert Consensus Decision Pathway for Optimization of Heart Failure Treatment: Answers to 10 Pivotal Issues About Heart Failure With Reduced Ejection Fraction: A Report of the American College of Cardiology Solution Set Oversight Committee," *Journal of the American College of Cardiology*, vol. 77, no. 6, pp. 772–810, 2021.